Journal of Neurochemistry

JOURNAL OF NEUROCHEMISTRY | 2017 | 142 | 464–477 doi: 10.1111/jnc.14068

ORIGINAL ARTICLE

Astrocytes contribute to Aβ-induced blood–brain barrier damage through activation of endothelial MMP9

Simona Federica Spampinato,* Sara Merlo,* Yasuteru Sano,† Takashi Kanda† and Maria Angela Sortino*

*Department of Biomedical and Biotechnological Sciences, Section of Pharmacology, University of Catania, Catania, Italy

†Department of Neurology and Clinical Neuroscience, Yamaguchi University Graduate School of Medicine, Ube, Yamaguchi, Japan

Abstract

The blood–brain barrier (BBB) plays an important role in the maintenance of the brain homeostasis, and its proper functions are warranted by the interplay between different cellular components (endothelial cells, astrocytes and pericytes). BBB dysfunctions in pathological conditions, and particularly in Alzheimer's disease, have been documented. Here, using an *in vitro* BBB model, the interaction between endothelial cells and astrocytes exposed to Aβ1-42 was investigated. Human endothelial cells, cultured in monolayer or co-cultured with astrocytes, were exposed to Aβ1-42 (2 μM for 18 h). Aβ induced dysfunction of endothelial barrier, as assessed by enhanced permeability to FITC-conjugated dextran and reduced expression of claudin-5; these modifications were observed in the co-culture model, but not in endothelial cells cultured in monolayer. Similarly, Aβ-induced damage at the barrier was observed when endothelial cells were challenged in the presence of conditioned medium generated by astrocytes previously exposed to Aβ (ACM Aβ). Endothelial barrier damages were associated with enhanced matrix metalloprotease 9 (MMP9) activity, known to mediate claudin-5 disruption. These events were not related to the direct effects played by Aβ on endothelial cells, but they were rather the consequence of Aβ-induced vascular endothelial growth factor (VEGF) expression in astrocytes. Indeed, when vascular endothelial growth factor expression was down-regulated in astrocytes, neither barrier properties or MMP9 expression in endothelial cells were affected after Aβ exposure both in the co-culture model or in the presence of ACM Aβ. These data point out the importance of astrocytes' mediation in inducing endothelial sensitivity to Aβ1-42.

Keywords: Alzheimer's disease, claudin-5, neurovascular unit, tight junctions, VEGF.

J. Neurochem. (2017) **142**, 464–477.

The blood–brain barrier (BBB) consists of specialized endothelial cells that, together with other components of the neurovascular unit (NVU; pericytes, astrocytes and neurons), preserve the proper environment in the central nervous system (CNS), restricting the entry of potentially harmful blood-borne agents, metabolites, drugs and immune cells into the CNS. Affections at the BBB functions have been often related to CNS pathological states. The involvement of the barrier in the initiation and perpetuation of multiple sclerosis is well documented (Ortiz *et al.* 2014), as well as of amyotrophic lateral sclerosis, Parkinson's disease and Huntington's disease (Capaldo and Nusrat 2009). Recently BBB involvement in Alzheimer's disease (AD) has been proposed. The progressive and irreversible cognitive decline that characterizes the disease is the consequence of beta amyloid (Aβ) accumulation and tau protein hyperphosphorylation that lead to neuronal degeneration, synaptic loss, plaque formation and gliosis. The leakage

Received December 23, 2016; revised manuscript received May 4, 2017; accepted May 4, 2017.

Address correspondence and reprint requests to Maria Angela Sortino, Department of Biomedical and Biotechnological Sciences, Section of Pharmacology, University of Catania, Catania 95123, Italy. E-mail: msortino@unict.it

Abbreviations used: ACM, astrocyte conditioned medium; AD, Alzheimer's disease; Aβ, β-amyloid; BBB, blood–brain barrier; CNS, central nervous system; DMSO, dimethylsulfoxide; FBS, fetal bovine serum; hAST, human astrocytes; MMP, matrix metalloproteinase; NVU, neuro vascular unit; TJ, tight junction; VEGF, vascular endothelial growth factor.

of the BBB has been often observed in patients with early AD (van de Haar *et al.* 2016), and post-mortem studies show coexisting cerebrovascular affections in AD patients (de la Torre 2002; Jellinger and Attems 2005; Keller 2013). Recent studies support the idea that BBB involvement in AD could precede neurodegenerative events (Bell and Zlokovic 2009; Zhao *et al.* 2015). The two-hit vascular hypothesis (Wang *et al.* 2014; Lamoke *et al.* 2015) proposes that endothelial dysfunction at the BBB, consequence of cerebrovascular damage, can be the first event leading to Aβ overload in the CNS (second hit), thus causing neurodegeneration (Sagare *et al.* 2012; Brkic *et al.* 2015). BBB dysfunction caused by Aβ challenge may result in impaired neuronal metabolic supply and reduced Aβ clearance through the barrier (Di Marco *et al.* 2015), thus increasing its load in the CNS. Aβ itself can affect endothelial properties. In *in vitro* BBB model, Aβ exposure induces the expression of adhesion molecules ICAM-1 and VCAM-1 (Liu *et al.* 2011), and modifies the distribution of tight junction (TJ) proteins, (Marco and Skaper 2006; Gonzalez-Velasquez *et al.* 2008; Nagababu *et al.* 2009). TJs are the main modulators of paracellular movement of solutes across endothelial barrier (Garcia *et al.* 2014) and in pathological states are considered as proper indicators of BBB structural modifications (Abbott *et al.* 2006; Zenaro *et al.* 2016). Astrocytes affect BBB function as they release several factors able to induce the formation of TJs, enhance the expression of transporters (Cheslow and Alvarez 2016) and modulate endothelial response to inflammatory stimuli. The role that astrocytes play in neurodegenerative disorders, such as AD, is still unclear. They can certainly reduce support of neuronal activities and release chemokines and cytokines [reviewed in (Garwood *et al.* 2016)] that can aggravate neuronal degeneration. Nevertheless, astrocytes can also play a protective role in models of neurodegeneration (Jo *et al.* 2014). Here, using an *in vitro* BBB model, we explored the interaction of astrocytes with endothelial cells after Aβ challenge. Human endothelial cells and astrocytes were either exposed to Aβ independently or in a more physiological condition in which direct interaction between the cells was enabled. The presence of astrocytes was essential to induce endothelial response to Aβ, resulting in increased barrier permeability and TJ disruption.

Materials and methods

All studies were carried out using cell lines and no institutional approval is required in this case.

Drugs and reagents

Cell culture plastics were provided by BD Falcon (Milan, Italy). Polycarbonate membrane transwell inserts, pores 3 μm, and collagen I rat tail were provided by Corning (Milan, Italy). MCDB-131 medium and fetal bovine serum (FBS) were from Invitrogen Srl (Milan, Italy). EGM-2 SingleQuotsTM was provided by Lonza, (Basel, Switzerland). Astrocyte medium was from ScienCell Research Laboratories (Carlsbad, CA USA). Beta amyloid (Aβ1-42) peptide (Innovagen, Lund, Sweden) was solubilized in dimethylsulfoxide as a 5 mM stock. For experiments, 100 μM Aβ(1-42) was aggregated by overnight incubation at 4°C followed by freeze-thaw cycles to be enriched in oligomers, as previously described (Merlo and Sortino 2012). GM6001 was from Merck (Merck Millipore, Darmstadt, Germany). The following primary antibodies were used: antirabbit Claudin-5 (1 : 200 for WB and 1 : 100 for ICC, Thermo Fisher Scientific Cat# 34-1600 RRID:AB_2533157, Milan Italy), anti-rabbit matrix metalloprotease 9 (MMP9; 1 : 800, Millipore Cat# AB19016 RRID:AB_91090), anti-rabbit MMP2 (1 : 700, SantaCruz Biotechnology, CA, USA sc-10736 RRID:AB_2250826), anti-rabbit vascular endothelial growth factor (VEGF) (1 : 400, Santa Cruz Biotechnology Cat# sc-152 RRID:AB_2212984), anti-rabbit beta-actin (1 : 2500, Sigma-Aldrich St Louis, MO, USA, Cat# A2066 RRID:AB_476693), anti-mouse alpha-tubulin (1 : 5000, Sigma-Aldrich, Cat# T9026 RRID:AB_477593).

Cell culture

TY-10 cells, an adult human brain microvascular endothelial cell line, were immortalized after transfection with plasmid expressing temperature sensitive Simian virus-40 large T-antigen (ts-SV40-LT) and the catalytic subunit of human telomerase, as previously described (Sano *et al.* 2010; Spampinato *et al.* 2015). TY-10 cells were grown in MCDB-131 media (Sigma-Aldrich) supplemented with EGM-2 SingleQuotsTM and 20% heat-inactivated FBS. Astrocytes (hAST), a human cell line, were immortalized after transfection with the same ts-SV40-LT, plasmid as previously described (Haruki *et al.* 2013), and were grown in astrocyte media containing 2% heat-inactivated FBS, astrocyte growth supplement and penicillin/streptomycin solution as provided with the Astrocyte media kit (ScienCell Research Laboratories). Both cell lines were developed at Yamaguchi University (Japan), in the labs of Dr Sano and Kanda. For experiments, both TY-10 cells and hAST were grown at 33°C until confluency was reached and then transferred at 37°C, where they exhibit growth arrest and differentiation. After 2 days of differentiation, cells were exposed to Aβ 1-42 for 18 h. To achieve astrocyte conditioned medium (ACM), astrocytes were exposed to either vehicle (ACM resting) or Aβ1-42, 2 μM (ACM Aβ), for 6 h, then washed and incubated with fresh medium for further 18 h. This particular paradigm was chosen in order to allow exposure of astrocytes to Aβ for a reasonable time to induce Aβ effects before removal so that transferred ACM did not contain any Aβ.

FITC-dextran permeability assay

In the monolayer model, endothelial cells were plated on collagen type-I-coated polycarbonate transwell tissue culture inserts (0.33 cm^2 inserts, 120 k/each) and regularly checked for confluency. In the co-culture model, hAST were seeded on 24 well plates (90 k/well). After 1 h polycarbonate transwell tissue culture inserts were transferred onto the same plates, TY-10 cells were plated on top of the insert (0.33 cm^2 inserts, 120 k/each) and grown in astrocyte medium. After 3 days at 33°C, cells were transferred at 37°C to allow cell differentiation for 2 more days. Treatments were performed when transendothelial electrical resistance (TEER) values were stable (34.05 ± 0.5 Ω cm^2, as

reported [Sano *et al.* 2013)]). After 18 h treatment, inserts were equilibrated in the "assay medium" (phenol red-free Dulbecco's modified Eagle's medium supplemented with 1% FBS) for 30 min at 37°C. Solute permeability was assessed using 10 kDa FITC-conjugated dextran (5 mg/mL Sigma-Aldrich). Dextran was applied to the luminal compartment. One hundred microliters of sample were collected from the abluminal compartment at different time points (30 and 60 min). The fluorescence of the sample was measured at 485/520 nm (excitation/emission) using Varioskan TM LUX multimode microplate reader (ThermoFisher, Milan, Italy). Fluorescence intensity values were plotted on the *Y*-axis and represented as % of control.

Immunocytochemistry

TY-10 cells were plated on collagen I rat tail-coated coverslips. When grown in co-culture, astrocytes plated on the transwell tissue culture inserts, were transferred on top of the endothelial monolayer. Cultures were checked for confluency and then kept for 2 days at 37°C before any kind of treatment, as indicated. After 18 h treatment, TY-10 cells were fixed in ice-cold acetone for 15 min and subsequently in ice-cold methanol for 20 min. Primary antibody, anti-rabbit Claudin-5 (1 : 100), was incubated in the presence of 0.1% Triton X-100 at 4°C overnight. Secondary antibody (Goat anti-rabbit Alexafluor 488, Molecular Probes Cat# A-11070 RRID: AB_142134) was incubated for 45 min at 25°C. 4′,6-Diamidino-2-phenylindole was used for counterstaining. Slides were imaged using an epifluorescent Zeiss Observer.Z1 microscope equipped with the Apotome.2 acquisition system connected to a digital camera. No blinding observation was performed in these analyses.

Western blot

Cells were harvested with M-PER mammalian protein extraction reagent (Thermofisher) supplemented with protease inhibitor, and protein concentration determined, using the Bradford reagent (Sigma-Aldrich). Thirty μg of each sample were separated by sodium dodecyl sulfate page and transferred to nitrocellulose membranes (Hybond ECL, Amersham Biosciences Europe GmbH, Milan, Italy). Membranes were blocked with Odyssey blocking buffer (LI-COR Biotechnology GmbH, Bad Homburg, Germany) diluted 1 : 1 with phosphate-buffered saline for 30 min and probed with the following primary antibodies overnight: anti-rabbit Claudin-5 (1 : 200; Thermo Fisher Scientific Cat# 34-1600 RRID: AB_2533157), anti-rabbit MMP9 (1 : 800; Millipore Cat# AB19016 RRID:AB_91090), anti-rabbit MMP2 (1 : 700; Santa-Cruz Biotechnology, sc-10736 RRID:AB_2250826), anti-rabbit VEGF (1 : 400; Santa Cruz Biotechnology Cat# sc-152 RRID: AB_2212984), anti-mouse alpha-tubulin (1 : 5000; Sigma-Aldrich Cat# T9026 RRID:AB_477593). Membranes were then processed for the immunodetection using specific fluorescent secondary antibodies IRDye®680 or IRDye®800-conjugated secondary antibodies (LI-COR). Detection of specific bands was carried out using the Licor Odyssey® Infrared Imaging System (LI-COR). Band intensity was analyzed, using the image processing software "Image J" developed by NIH and in public domain.

Subcellular protein fractionation

Separation and preparation of cytoplasmic and membrane protein extracts from endothelial cells were performed, using the subcellular protein fractionation kit for cultured cells (ThermoScientific) according to the manufacturer's instruction. Extracts obtained were then processed for western blotting after protein quantification using the Bradford reagent.

Qrt-pcr

Total RNA was extracted from cell cultures using the RNeasy plus Mini Kit (Qiagen, Milan). One μg of RNA was used for cDNA synthesis, using the Superscript-VILO kit (Invitrogen) according to manufacturer's instruction. Quantitative real-time PCR was performed with Rotor Gene Q using QuantiNova SYBR Green PCR Kit (Qiagen). The melting curves obtained after each PCR amplification reaction confirmed the specificity of the 2-[N-(3-dimethylaminopropyl)-N-propylamino]-4-[2,3-dihydro-3-methyl-(benzo-1,3-thiazol-2-yl)-methylidene]-1-phenyl-quinolinium (SYBR Green assays. The following primers were used: VEGF (F 5′-ATCTTCAAGCCATCCTGTGTGC-3′; R 5′- GAGGTTTGATC CGCATAATCTG-3′); Hs_RPLP0_1_SG QuantiTect Primer Assay (Qiagen, cat n. QT00075012). For MMP 9 and MMP 2 primers were exactly as described (Munaut *et al.* 2003).

Gelatin zymography assay

Equal amount of endothelial medium in non-reducing conditions were separated in an 8% sodium dodecyl sulfate-polyacrylamide gel containing 0.1% porcine skin gelatin (300 bloom, Sigma-Aldrich, Milan, Italy). The gel was washed in renaturing buffer (2.5% Triton X-100) for 45 min at 25°C. Then it was incubated with zymography development buffer (Bio-Rad Laboratories, Milan, Italy) for 45 min at 25°C and maintained in fresh zymography development buffer for 22 h at 37°C. Finally the gel was stained with 0.25% R-250 Coomassie solution (Sigma; 30 min at 25°C) and destained in a 2 : 1 methanol:acetic acid solution (30 min at 25°C). Odyssey scanner was used to acquire digital scan of the gels. Images were subjected to densitometric analysis with the aid of the Image J processing software.

VEGF silencing

Cultured astrocytes were transfected with lipofectamine 2000 (Invitrogen) and either negative control or VEGF siRNA (1.5 pM; Santa Cruz). Incubation was carried out in Optimem medium for 6 h at 37°C, and let to recover in complete astrocyte medium for 18 h. Endothelial cells were then co-cultured with astrocytes for 24 h and co-cultures were exposed to treatment for further 18 h.

Statistical analysis

Data shown are always mean ± SEM of 3–7 independent experiments each run in triplicates or quadruplicates. Data were analyzed by Student's *t*-test or by one-way ANOVA followed by Newman–Keuls test for significance when three or more conditions were compared. Here $p < 0.05$ was taken as the criterion for statistical significance.

Results

Astrocytes influence Aβ effects at endothelial level

Human brain microvascular endothelial cell monolayer (TY-10 cells) was exposed to 2 μM Aβ1-42 for 18 h and barrier

properties were investigated. Paracellular diffusion was evaluated by the measure of endothelial permeability to 10 kDa FITC-conjugated dextran. Exposure to 2 μM Aβ1-42 was not able to induce any variation in dextran diffusion at the time point examined (30 min; Fig. 1a). Observation was prolonged at longer time points (up to 120 min), but no changes were detectable (Data S1a and b). TY-10 cells were then co-cultured with human astrocytes (hAST) and exposed to 2 μM Aβ1-42 for 18 h; in this set of experiments, the amount of the dye-conjugated molecule going through the endothelial monolayer was significantly increased after 30 min of exposure to dextran (Fig. 1b). This increase was maintained at later time points (60 and 120 min, Fig. S1c and d). The higher permeability was not consequence of cell death: Aβ1-42 did not modify in fact viability of either endothelial cells or astrocytes (Data S2).

Increased paracellular permeability was accompanied by modifications in the structure of TJ. The expression of claudin-5, the main constituent of TJ, was assessed after Aβ1-42 challenge. When the endothelial monolayer was exposed to 2 μM Aβ1-42 for 18 h no variations in the expression of claudin-5 were detected (Fig. 2a). However, immunocytochemical analysis showed that claudin-5, which was mostly localized at the cell boundaries under resting conditions (control), was altered following Aβ1-42 treatment resulting in its intracellular redistribution (Fig. 2b, indicated by asterisks). In contrast, when endothelial cells were grown in co-culture with astrocytes and exposed to 2 μM Aβ1-42 for 18 h, the treatment significantly reduced the expression of claudin-5 (Fig. 2c) and the intracellular redistribution of claudin-5 was more diffuse (compare asterisks between Fig. 2b and d). Moreover, the cell to cell junctions were loosened (white arrows in Fig. 2d). To further verify Aβ-induced TJ redistribution inside the cell, subcellular protein fractionation was performed. Cytoplasmic and membrane fractions were isolated and the expression of claudin-5 was evaluated. The total amount of claudin-5 expressed in the cytoplasmic fraction was increased by Aβ treatment (Fig. 2e), while the expression of claudin-5 localized at the membrane was significantly reduced (Fig. 2f).

Astrocyte-released soluble factors modulate Aβ effects at endothelial level

The reported data prompted us to investigate whether soluble factors produced by astrocytes could affect endothelial response to Aβ. Astrocytes conditioned medium (ACM) was generated by cultures exposed to vehicle or Aβ1-42 for 6 h, and collected after 18 h of recovery (ACM resting and ACM Aβ, respectively). Endothelial exposure to either ACM resting or Aβ failed to modify FITC-conjugated dextran permeability (Fig. 3a). Endothelial cells were subsequently exposed to Aβ1-42, 2 μM, in the presence of media released by either resting (ACM resting) or Aβ-challenged (ACM Aβ) astrocytes. In the presence of ACM resting, Aβ treatment did not modify endothelial properties (Fig. 3b), whereas ACM Aβ increased endothelial sensitivity to Aβ challenge (Fig. 3c). Accordingly, the expression of claudin-5 was not affected when endothelial cells were exposed to ACM either

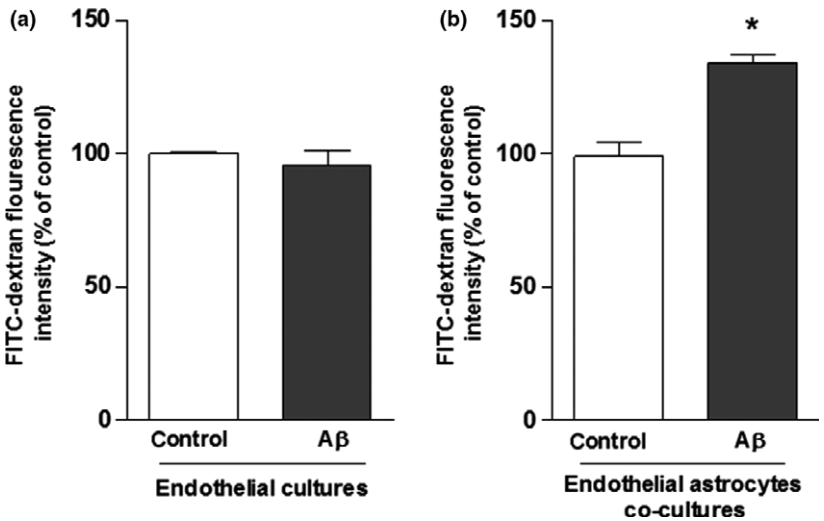

Fig. 1 Aβ1-42 affects endothelial permeability only in the presence of astrocytes. Endothelial cultures were exposed to Aβ1-42 (Aβ) 2 μM for 18 h. Endothelial properties were evaluated measuring FITC-conjugated dextran permeability through the monolayer, 30 min after addition of the dye (a). Endothelial cells were co-cultured with astrocytes and exposed to Aβ 2 μM for 18 h before permeability assay was performed (b). Monolayer permeability is expressed as percentage of control of FITC-dextran-10 kDa fluorescent intensity, plotted on the *Y*-axis. Values represent mean ± SEM of 3 (a) and 4 (b) independent experiments. *$p < 0.05$ versus control. Significance was assessed by Student's *t* test.

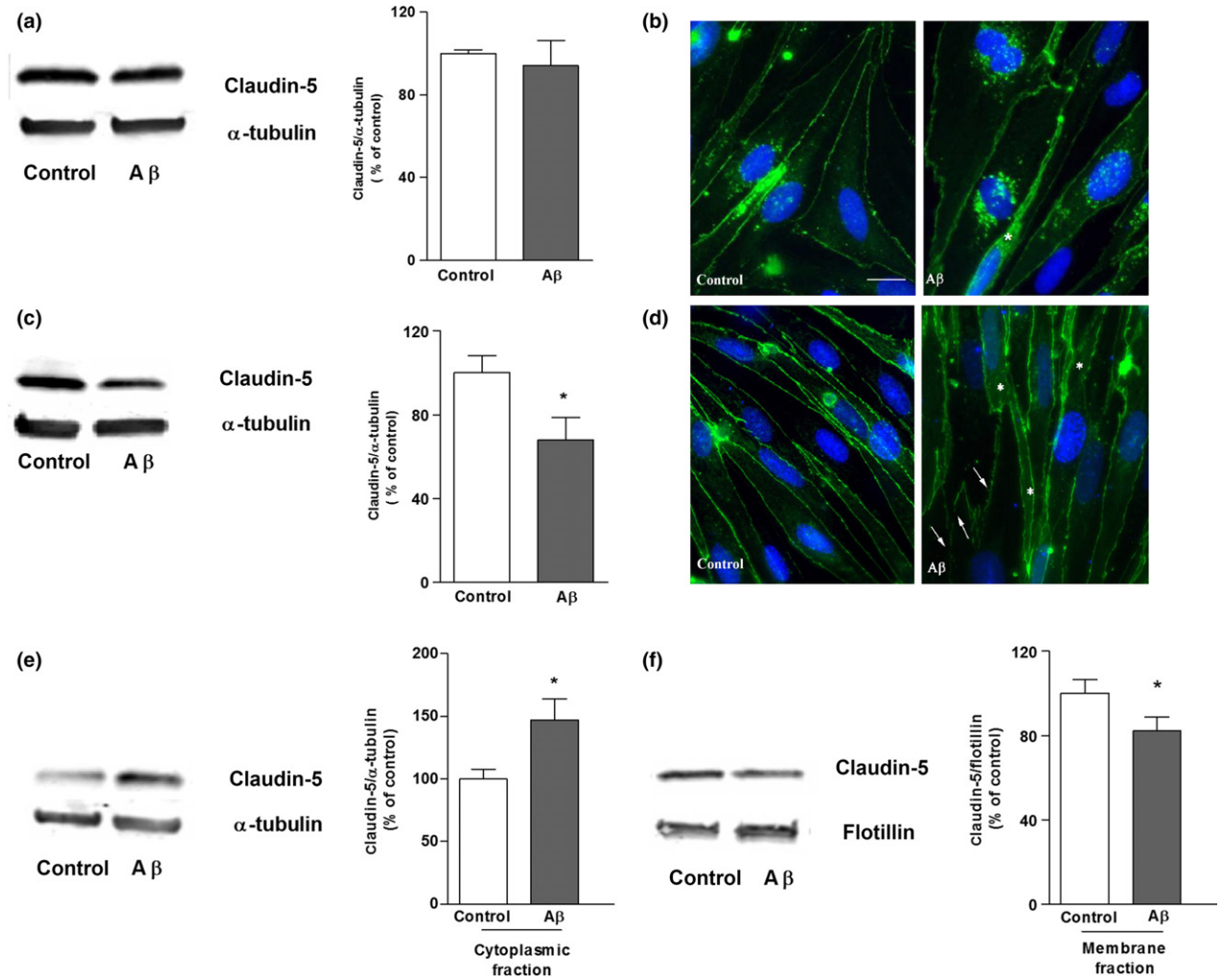

Fig. 2 Changes of claudin-5 expression are induced by Aβ1-42 treatment only in endothelial astrocytes co-cultures. Endothelial cultures were exposed to Aβ 2 μM for 18 h. The expression (a) and localization (b) of claudin-5 were evaluated by western blot and immunofluorescence analysis. Endothelial astrocytes co-cultures were exposed to Aβ 2 μM for 18 h before western blot (c) and immunofluorescence analysis (d). Claudin-5 localization at the cytosolic (e) or membrane (f) compartment after Aβ treatment was evaluated by western blot of proteins derived from subcellular fractionation. In the membrane compartment, the expression of flotillin was used as loading control. Values are expressed as percent of control. Data are mean ± SEM of 4 (a and c) and 6 (e and f) experiments. *$p < 0.05$ versus control. Significance was assessed by Student's *t*-test. In the histology panels white arrows show the areas in which claudin-5 localization at the boundaries is reduced, while asterisks indicate cytosolic translocation. Claudin-5 is represented in green, while 4′,6-diamidino-2-phenylindole (DAPI) is used to counter-stain nuclei. Scale bar represents 10 μm

from resting or Aβ challenged astrocytes (Fig. 3d), but when endothelial cells were challenged with Aβ in the presence of ACM Aβ, the expression of claudin-5 was significantly reduced (Fig. 3e). The cellular localization of the protein was as well modified in these conditions: Aβ treatment induced claudin-5 translocation from the cell boundaries, reducing cell to cell contact (arrows in Fig. 3f); the increased localization of the protein at the cytosolic fraction (Fig. 3g) was confirmed by western blot analysis that showed also a reduction in membrane-localized claudin-5 (Fig. 3h) after Aβ challenge.

Aβ induces the expression of VEGF in astrocytes

Among all the factors that astrocytes release upon Aβ1-42 activation, attention was focused on VEGF. After exposure of astrocytes to 2 μM Aβ1-42, both VEGF mRNA and protein levels were increased. The mRNA peak was significantly reached after 6 h of Aβ exposure (Fig. 4a) while the protein levels were increased 18 h after treatment (Fig. 4b). Exposure to 100 ng/mL VEGF for 18 h increased endothelial permeability to FITC-conjugated dextran (Fig. 4c) and significantly reduced expression of claudin-5 (Fig. 4d). VEGF expression in astrocytes was reduced, using a short

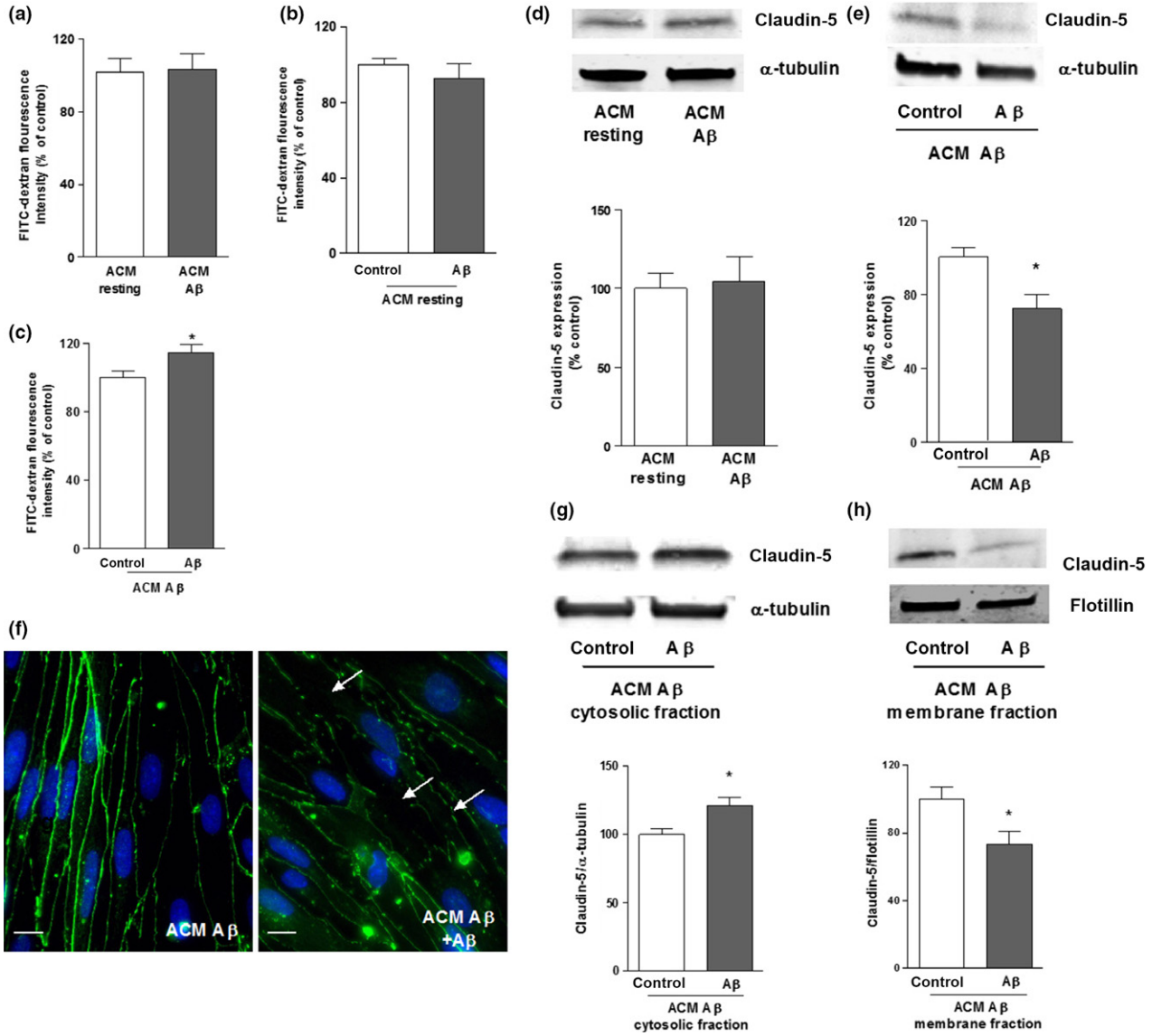

Fig. 3 Conditioned media collected from Aβ-treated astrocytes increase endothelial sensitivity to Aβ. Endothelial cells were exposed to conditioned medium released by either resting [astrocyte conditioned medium (ACM resting)] or Aβ1-42 (ACM Aβ, 2 μM) challenged astrocytes. Endothelial permeability to FITC-conjugated dextran was evaluated (a). Endothelial monocultures were exposed to Aβ1-42 (Aβ, 2 μM) in the presence of either ACM resting (b) or ACM Aβ (c). and endothelial permeability to FITC-conjugated dextran was evaluated after 30 min (b and c). Total claudin-5 expression was evaluated in endothelial cultures exposed to ACM resting or ACM Aβ (d) and further challenged with Aβ1-42 2 μM for 18 h (e). Panel f shows immunofluorescence of claudin-5 in endothelial cultures exposed to Aβ in the presence of ACM Aβ. Western blot analysis of claudin-5 in the cytosolic (g) and membrane (h) fractions of endothelial cultures exposed to Aβ 1-42 in the presence of ACM Aβ is reported in panels g and h. Monolayer permeability is expressed as percent of control of FITC-dextran-10 kDa fluorescent intensity. Values are expressed as percent of control. Data are mean ± SEM of 3 independent experiments. *$p < 0.05$ versus control. Significance was assessed by Student's *t*-test. In the images white arrows indicate the regions in which the protein localization at the boundaries was discontinued. Claudin-5 is represented in green, while 4′,6-diamidino-2-phenylindole (DAPI) is used to counter-stain nuclei. Scale bar represents 10 μm.

interfering RNA (VEGF siRNA), yielding a marked down-regulation of VEGF mRNA expression 24 h after transfection (Fig. 5a). This effect was still maintained at 48 h when both RNA levels (Fig. 5a) and protein expression (Fig. 5b) were significantly reduced. Endothelial cells were therefore co-cultured with astrocytes expressing lower VEGF levels, and exposed to 2 μM Aβ1-42 for further 18 h. After Aβ challenge, endothelial permeability to FITC-conjugated dextran was significantly reduced when compared to co-cultures in which astrocytes were exposed to control siRNA

(scramble) (Fig. 5c). The expression of claudin-5 was evaluated in endothelial cells co-cultured with astrocytes expressing lower VEGF levels (siRNA VEGF); in this case, the expected reduction in claudin-5 expression after Aβ challenge was not observed (Fig. 5d). Immunocytochemistry analysis showed that the protein localization at the cell boundaries was still well defined after Aβ challenge when endothelial cells were co-cultured with siRNA VEGF astrocytes (Fig. 5e).

Astrocyte-mediated endothelial leakage requires MMP9

MMPs are known for their ability to induce TJ degradation. Their expression and activity were thus investigated in this model. MMP9 was significantly increased in endothelial cells co-cultured with astrocytes, after 18 h of exposure to 2 μM Aβ1-42. MMP2 expression, in contrast, was only slightly but not significantly modified by the treatment (Fig. 6a). However, when Aβ1-42 was added directly to the endothelial monolayer, increased expression of MMP2, but not of MMP9, was observed (Fig. 6b). Further, no modifications in the expression of MMP2 and MMP9 were observed in astrocytes exposed to Aβ1-42 (Fig. S3). Since the co-culture model is the one in which we observed barrier modification after Aβ exposure, we first analyzed MMP9 activity, in this condition, by gel zimography. The activity of MMP9 released in the media was significantly increased after Aβ treatment (Fig. 6c). In contrast, although a trend to an increase in MMP9 active form was observed, significance was not achieved when Aβ was added directly to endothelial cultures (Fig. 6d). However, when endothelial cells were exposed to Aβ in the presence of ACM Aβ, the expression of MMP9 in response to Aβ insult was again mostly affected (Fig. 6e–g). Here Aβ treatment induced in fact a significant up-regulation of MMP9 gene (Fig. 6e) and protein (Fig. 6f) expression and the enzymatic activity was increased as well (Fig. 6g). MMP2 expression instead was not significantly

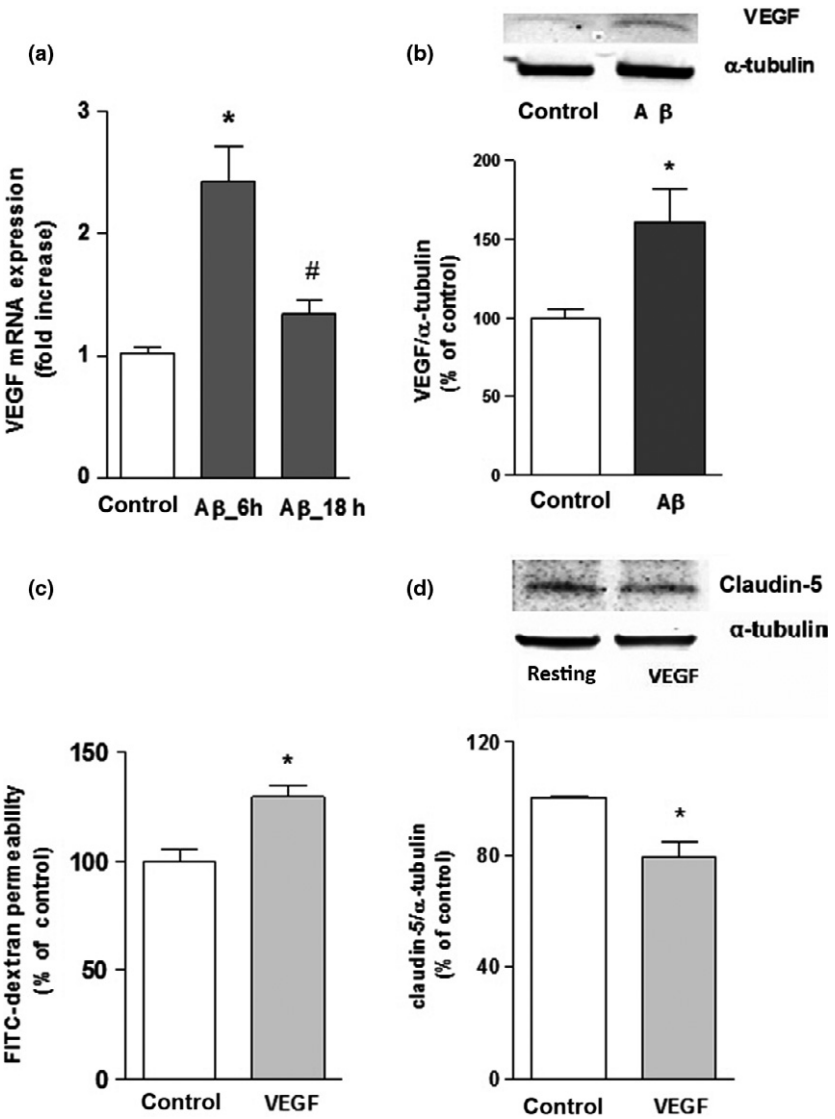

Fig. 4 Vascular endothelial growth factor (VEGF) simulates the response of endothelial cells to Aβ in the presence of conditioned medium from Aβ-treated astrocytes. VEGF mRNA levels were evaluated after 6 and 18 h; whereas VEGF protein expression was evaluated after 18 h Aβ (2 μM) treatment (b). Exposure of endothelial cells to VEGF (100 ng/mL for 18 h) modified FITC-conjugated dextran permeability (c) as well as the expression of claudin-5 (d). Values are expressed as percent of control. Data are mean ± SEM of 3 experiments. *$p < 0.05$ versus control and #$p < 0.05$ vs Aβ_6 h. Significance was assessed by one way ANOVA, followed by Newman-Keuls test (a) and Student's *t*-test (b–d).

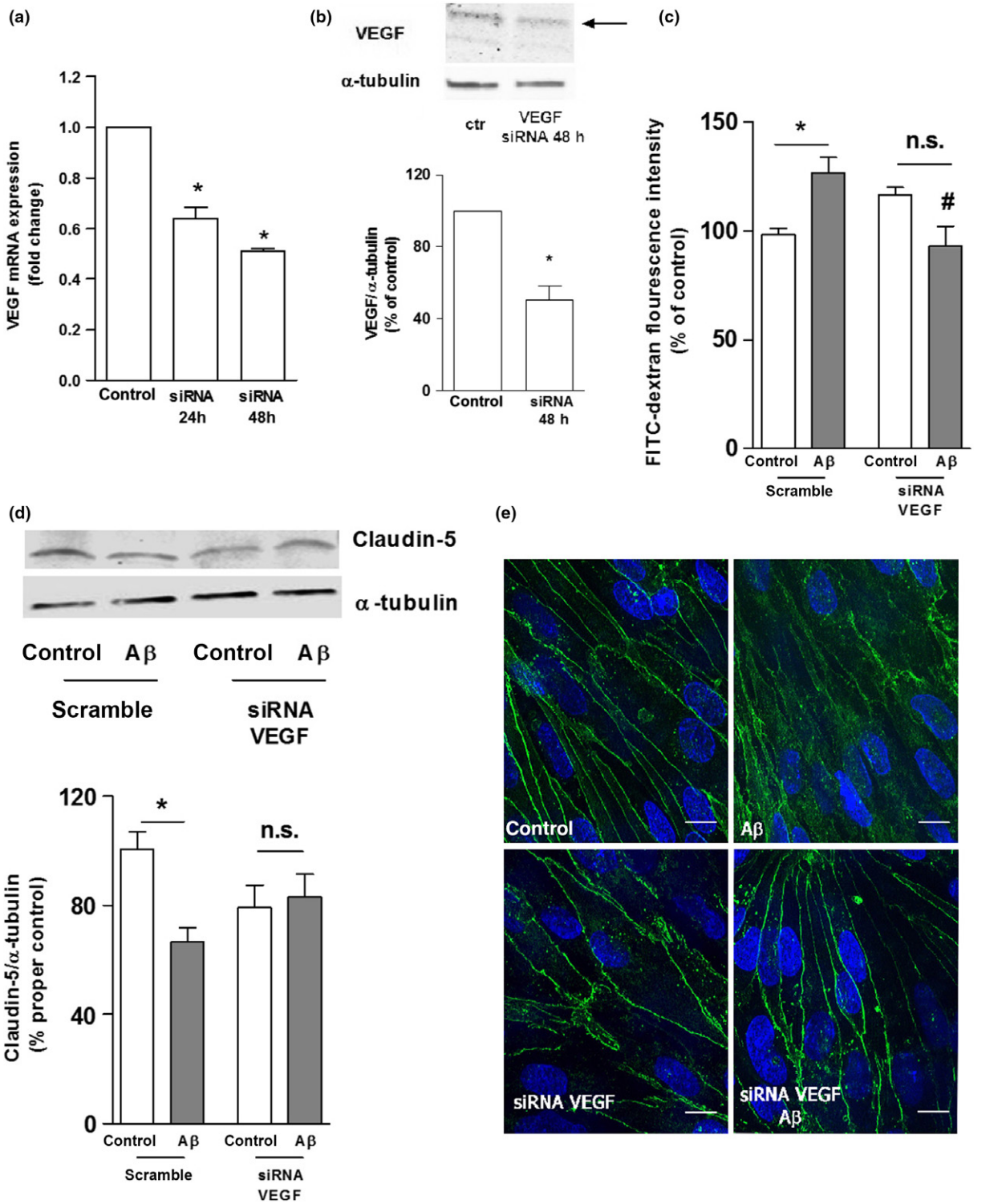

Fig. 5 Down-regulation of the expression of vascular endothelial growth factor (VEGF) in astrocytes prevents Aβ effects on endothelial properties. The expression of VEGF in astrocytes was selectively reduced by incubation with VEGF siRNA (1.5 pM) as shown by a time-dependent reduction in mRNA (a) and decreased protein expression detected at 48 h (b). Endothelial cells were co-cultured with control (scramble) or VEGF-silenced (siRNA VEGF) astrocytes and then exposed to Aβ 2 μM for 18 h. Both endothelial permeability (c) and claudin-5 expression (d) and localization (e) are shown. Scale bar represents 10 μm. Data are mean ± SEM of 3 (a and b) and 7 (c and d) experiments. *$p < 0.05$ vs. control and #$p < 0.05$ vs. Aβ scrambe). Significance was assessed by Student's *t*-test (b) and one way ANOVA, followed by Newman-Keuls test (a, c and d).

Fig. 6 Astrocytes are necessary to induce MMP9 expression and activity in endothelial cells after Aβ1-42 treatment. The expression of MMP2 and MMP9 in endothelial cells co-cultured with astrocytes (a) or in monolayer (b) was assessed by western blot analysis following exposure to Aβ 2 μM for 18 h. The medium released by endothelial cells following exposure to Aβ either in the presence of astrocytes (c) or in monoculture (d) was subjected to gelatin zymography assay to evaluate MMP9 enzymatic activity. Expression of MMP9 was analyzed in endothelial cells exposed to Aβ in the presence of Aβ astrocyte conditioned medium (ACM) by qRT-PCR (e) and western blot (f). The release and activity of the protease was evaluated by processing endothelial culture media in a gelatin zymography assay (g). Values are expressed as percent of control. Data are mean ± SEM of 3 (a, c, d and g) and 6 (b and f) experiments. $*p < 0.05$ versus proper control. Significance was assessed by Student's *t*-test.

affected, as indicated by gene expression, protein levels and enzymatic activity (Fig. S4).

Endothelial astrocytes co-cultures were then exposed to the broad spectrum MMP inhibitor GM6001 (5 μM) and challenged with Aβ1-42 for 18 h. GM6001 was able to prevent both the enhanced permeability (Fig. 7a) and the reduced claudin-5 expression (Fig. 7b) induced by Aβ1-42. Similarly, when endothelial cells were exposed to ACM Aβ and treated with GM6001, the drug was able to prevent claudin-5 reduction induced by Aβ insult (Aβ+GM6001). The MMP inhibitor alone did not modify the expression of the protein (Fig. 7c). Finally, the expression of MMP9 in endothelial cells co-cultured with siRNA VEGF astrocytes was investigated. Under these conditions, Aβ-induced increase in MMP9 expression was prevented (Fig. 7d).

Discussion

The BBB is a complex network in which endothelial properties are strongly affected by other components of the neurovascular unit (NVU). Pathological events may modify these interactions: in inflammatory conditions, for instance, astrocytes can affect endothelial properties by releasing cytokines (Nair *et al.* 2008) albeit they can also support BBB integrity (Mizee *et al.* 2014). The role of astrocytes in neurodegeneration/neuroprotection in AD has been long debated too (Batarseh *et al.* 2016; Ries and Sastre 2016), but their possible influence on BBB integrity has not been fully investigated. In our model, we wanted to evaluate whether endothelial barrier properties after Aβ stimulation could be affected by the presence of astrocytes. Indeed, in our conditions, endothelial monolayer was not sensitive to Aβ insult, albeit barrier leakage appeared when endothelial cells were exposed to Aβ in the presence of astrocytes themselves or in the presence of ACM Aβ. Previous studies have shown a direct effect of Aβ on endothelial permeability and/or on TJ expression, but such effects were always observed in the presence of much higher Aβ concentrations (up to 20 μM) (Marco and Skaper 2006; Tai *et al.* 2010; Gheorghiu *et al.* 2014) or in different *in vitro* models, like the retinal pigment epithelium (Park *et al.* 2014a) or choroid plexus epithelial cells (Brkic *et al.* 2015). Alternatively, the effect of Aβ (Aβ1-42 oligomers, 10 μM) was associated with decreased endothelial cell viability (Wan *et al.* 2015). At the low concentration we used, Aβ was not able to induce either endothelial or astrocytes' death, but it presumably induced astrocytes to release soluble factor/s that could increase endothelial sensitivity to Aβ itself. Our interpretation is supported by the observation that a similar effect by Aβ was observed in the presence not only of astrocytes, but also of conditioned medium from Aβ-pretreated astrocytes. The media released by Aβ-challenged astrocytes, *per se*, did not induce endothelial damage: the properties of endothelial cells exposed to ACM Aβ did not differ in fact from the condition in which they were exposed to ACM from resting astrocytes. An endothelial direct insult seems necessary to induce barrier properties modifications. Hence, astrocyte-released factor/s played a role in increasing endothelial sensitivity to Aβ. Of note, disruption of membrane properties, either in the co-culture system or in the presence of ACM Aβ, was not only because of a redistribution of claudin-5 from the membrane to the cytosolic compartment, but also due to an overall reduction in claudin-5 expression. The two effects do not exclude each other and they seem to occur concomitantly. Modulation by astrocytes of endothelial response to Aβ is not new. It has been shown, for instance, that the ability of Aβ to down-regulate endothelial P-glycoprotein expression is reverted by astrocytes (Park *et al.* 2014b). Also pericytes, the third component of the NVU, can modulate responses of endothelial cells, as shown by their attenuation of Aβ-induced changes of BBB properties (Park *et al.* 2016), further strengthening the concept of a strict interaction among different cellular components at the BBB. Among soluble astrocytic factors able to modulate endothelial properties (Abbott *et al.* 2006), one of the most interesting appeared VEGF that, besides its essential role in angiogenesis (Koch *et al.* 2011), is released by reactive astrocytes upon inflammatory stimuli (Maharaj and D'Amore 2007; Argaw *et al.* 2012) and induces down-regulation of TJ protein expression thus causing barrier permeability (Chapouly *et al.* 2015). In AD, VEGF is over-expressed in reactive astrocytes connected to blood vessels, via their endfeet, in proximity to perivascular Aβ plaques (Thirumangalakudi *et al.* 2006; Dal *et al.* 2014). Interestingly, Aβ injection in animals caused VEGF immunoreactivity in astrocytes, but not in endothelial cells (Zand *et al.* 2005). In our model, we confirmed that Aβ challenge, as previously suggested (Zand *et al.* 2005; Dal *et al.* 2014), induces higher VEGF expression in astrocytes and identified VEGF as an essential factor in astrocyte/endothelium interplay. Under

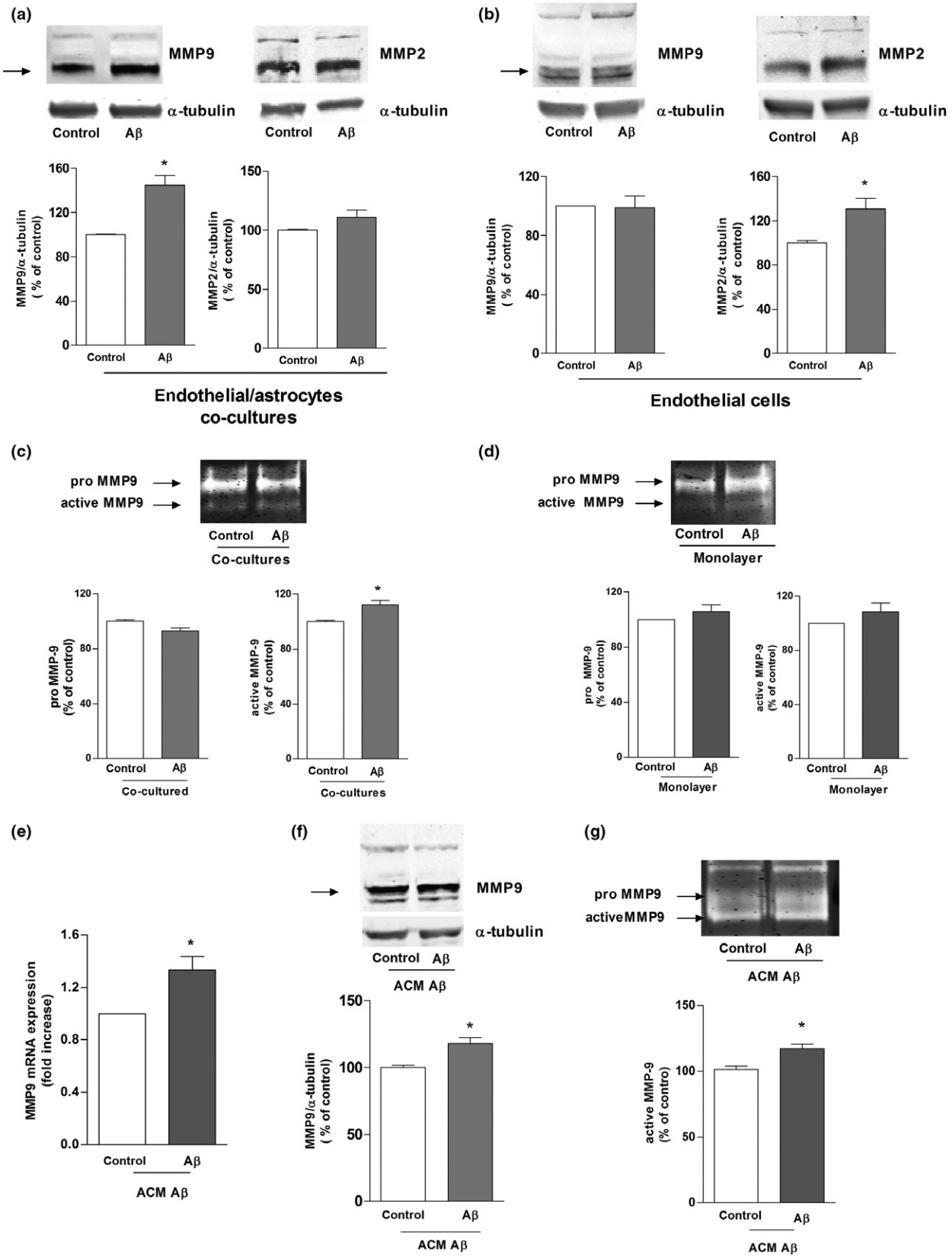
(a)
MMP9
α-tubulin
Control
Aβ
MMP2
α-tubulin
Control
Aβ
MMP9/α-tubulin (% of control)
MMP2/α-tubulin (% of control)
Endothelial/astrocytes co-cultures
(b)
MMP9
α-tubulin
Control
Aβ
MMP2
α-tubulin
Control
Aβ
MMP9/α-tubulin (% of control)
MMP2/α-tubulin (% of control)
Endothelial cells
(c)
pro MMP9
active MMP9
Control
Aβ
Co-cultures
pro MMP-9 (% of control)
active MMP-9 (% of control)
Co-cultured
Co-cultures
(d)
pro MMP9
active MMP9
Control
Aβ
Monolayer
pro MMP-9 (% of control)
active MMP-9 (% of control)
Monolayer
Monolayer
(e)
MMP9 mRNA expression (fold increase)
Control
Aβ
ACM Aβ
(f)
MMP9
α-tubulin
Control
Aβ
ACM Aβ
MMP9/α-tubulin (% of control)
ACM Aβ
(g)
pro MMP9
activeMMP9
Control
Aβ
ACM Aβ
active MMP-9 (% of contro)
ACM Aβ

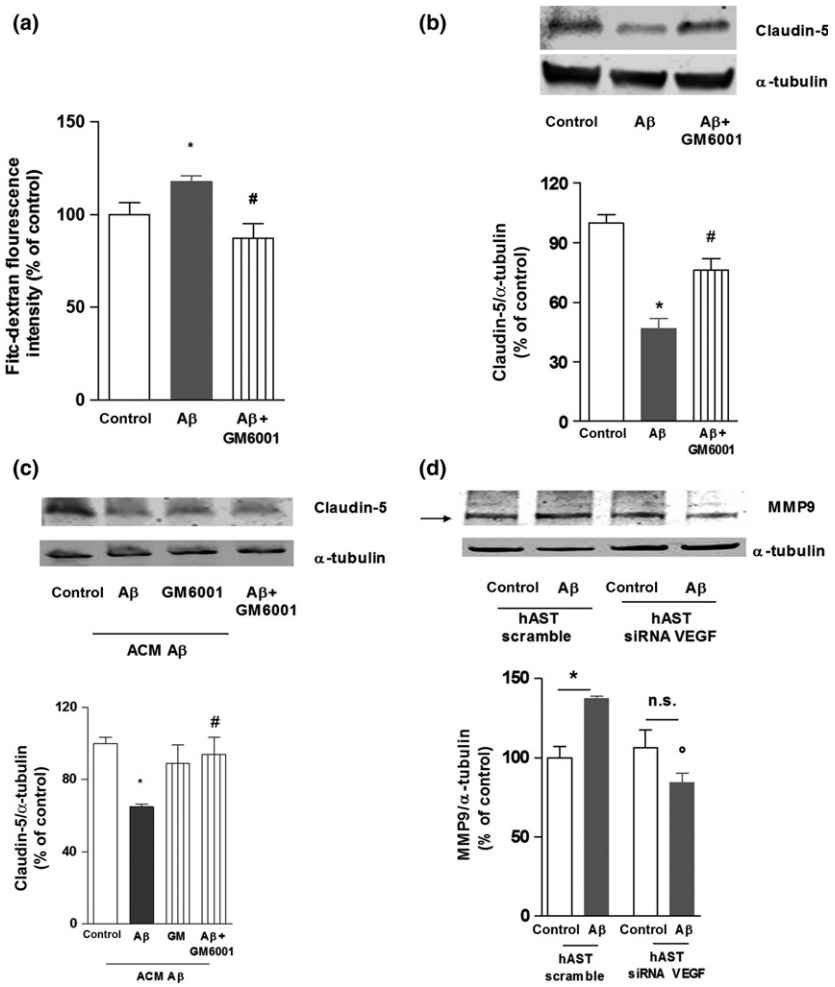

Fig. 7 MMP9 mediates Aβ effects on blood brain barrier (BBB) properties. Endothelial astrocytes co-cultures were exposed to Aβ 2 μM in association with GM6001 (5 μM). The permeability to FITC-conjugated dextran (a) and expression of claudin-5 were evaluated after 18 h (b). Claudin-5 expression was evaluated in endothelial cells exposed to conditioned medium from Aβ-treated astrocytes [astrocyte conditioned medium (ACM) Aβ] and challenged with Aβ 2 μM for 18 h in the presence of GM6001 (5 μM) (c). Aβ-induced MMP9 expression in endothelial co-cultured with astrocytes in resting condition (hAST scramble) or with reduced vascular endothelial growth factor (VEGF) expression (hAST SiRNA VEGF) was evaluated (d). Monolayer permeability is expressed as percentage of control of 10 kDa FITC-conjugated dextran fluorescent intensity. Values are expressed as percent of control. Data are mean ± SEM of 3 (a) or 6 (b, c and d) experiments, *$p < 0.05$ versus control, #$p < 0.05$ versus Aβ, °$p < 0.05$ versus Aβ hAST scramble. Significance was assessed by one-way ANOVA and Newman-Keuls test.

conditions of VEGF down-regulation, in fact, changes in barrier properties induced by Aβ exposure, in terms of both permeability and TJ expression, were not observed anymore.

MMPs have been associated with VEGF effects as shown in *in vivo* and *in vitro* models (Valable *et al.* 2005; Hollborn *et al.* 2007). Our attention was then focused on MMPs, as justified also by the fact that claudin-5 is a substrate for MMP2 and MMP9 (Fujimoto *et al.* 2008). Accordingly, the involvement of MMPs in the degradation of TJs and the components of basal lamina has been demonstrated in several neurological conditions (Yang *et al.* 2007, 2013; Xin *et al.* 2012; Tasaki *et al.* 2014; Kim *et al.* 2015). MMPs are implied in AD pathogenesis as well (Capaldo and Nusrat 2009), and in particular their involvement in BBB damage has been proposed (Kook *et al.* 2012; Park *et al.* 2014b; Zenaro *et al.* 2016). Furthermore, *in vitro* evidence supports MMP activities in TJ degradation induced by Aβ both at the BBB (Wan *et al.* 2015) and at the blood-cerebrospinal fluid barrier (Brkic *et al.* 2015).

We observed an increased expression of MMP9 following Aβ challenge only when endothelial cells were exposed to astrocytes, either in co-culture or after conditioned medium transfer. MMP9 enzymatic activity was then assessed in released medium by gel zymography. Data obtained confirmed that increased MPP9 activity in endothelial cells was related to the influence of astrocytes. These data apparently contrast with recent findings demonstrating a direct effect of Aβ on the expression and activity of both MMP2 and MMP9 directly in endothelial cells. However, again, only isolated oligomers of Aβ1-42 were used in that study and this can justify this discrepancy (Wan *et al.* 2015). In addition, we could detect a slight increase in MMP2 expression when endothelial cells were directly exposed to Aβ, an effect that cannot be excluded to occur, under appropriate conditions. Modifications in barrier properties were prevented when the non-specific MMP inhibitor, GM6001, was added to the astrocyte-endothelium co-culture. However, to dissect the cellular source of MMP mediating this effect, GM6001 was added only to endothelial cells exposed to Aβ in the presence of ACM Aβ. When added in the presence of ACM Aβ, the MMPs inhibitor did not modify basal expression of claudin-5, while it prevented the expected reduction in the protein induced by Aβ treatment,

pointing out the central role played by endothelial MMPs in this effect. As known, inhibition by GM6001 is not selective and an involvement of MMP2 or other MMPs cannot be ruled out. Interestingly, i.c.v. injection of Aβ1-42 oligomers produced, in choroid plexus epithelial cells, increased expression of several MMPs, including MMP9, likely responsible for loss of blood-CSF barrier integrity (Brkic *et al.* 2015). Enhanced leakage was prevented by the broad spectrum MMP inhibitor, but also in MMP3$^{-/-}$ deficient mice, suggesting a prominent role, specifically for MMP3, in Aβ1-42 oligomers-induced damage at the blood-CSF barrier (Brkic *et al.* 2015). Very recently, a major role in BBB microvascular hyperpermeability has been instead recognized to MMP9, as shown by prevention of BBB disruption under conditions of MMP9 inhibition by pharmacological or molecular tools, *in vitro* and *in vivo* (Alluri *et al.* 2016).

In order to find a link between astrocyte-derived VEGF and MMP9 activation, with ensuing enhanced endothelium permeability, the same experiments were performed under conditions of VEGF down-regulation in astrocytes. This caused prevention of Aβ effects on MMP9 expression and barrier properties, reinforcing the concept that VEGF represents the, or one of the, critical factor/s mediating astrocyte/endothelial cells interplay in this protocol.

The importance of the interplay between the different components of the NVU cannot be denied. In physiological conditions astrocytes strongly affect endothelial properties, thus reinforcing BBB. However, also in pathological conditions, as we observed in our system, astrocytes/endothelial communication influences barrier functions. The involvement of astrocytes, important to induce endothelial sensitivity to low Aβ challenge, is likely to occur in a more complex *in vivo* system, in which Aβ accumulation in the CNS can modify astroglial activity; these events lead to increased BBB damage that eventually may induce the infiltration of molecules and immune cells that participate to neuronal degeneration in AD. Astrocytes modifications induced by endothelial cells, on the other hand, cannot be excluded, further pointing out that the NVU is a complex network in which the interaction of all the components affects their response to physiological and pathological stimuli.

In conclusion, our results demonstrate that astrocytes are primarily involved in the toxic effects of Aβ at the BBB. A detailed knowledge of factors of astrocytic origin and pathways activated at the endothelial level as mediators of this cellular interplay, may help to identify new targets for prevention of Aβ-induced BBB damage.

Acknowledgments and conflict of interest disclosure

This work was supported by personal grants to Maria Angela Sortino (University of Catania cod. 20130143075). There is no conflict of interest to declare.

All experiments were conducted in compliance with the ARRIVE guidelines.

Supporting information

Additional Supporting Information may be found online in the supporting information tab for this article:

Figure S1. Modification in endothelial permeability induced by Aβ treatment. Endothelial cultures were exposed to Aβ1-42 (Aβ) 2 μM for 18 h. Endothelial properties were evaluated measuring FITC-conjugated dextran permeability through the monolayer, 60 and 120 min after addition of the dye (a and b). Endothelial cells were co-cultured with astrocytes and exposed to Aβ 2 μM for 18 h before permeability assay was performed; dextran permeability through the insert was evaluated 60 and 120 min after addition of the dye (c and d). Monolayer permeability is expressed as percentage of control of FITC-dextran-10 kDa fluorescent intensity. Values represent mean ± SEM of 3–4 independent experiments.*$p < 0.05$ versus control. Significance was assessed by Student's *t* test.

Figure S2. Concentration response curve of Ab on endothelial and astrocytes viability. Astrocytes (a) and endothelial cells (b) were exposed to increasing concentrations of Aβ 1-42 (0.5, 2, 5 μM) for 24 h. MTT assay was performed to evaluate cell viability. The concentration of 2 μM was not able to modify either endothelial or astrocytes viability and was used for all the described experiments., *$p < 0.05$ versus control. Significance was assessed by one-way ANOVA and Newman-Keuls test.

Figure S3. Aβ treatment did not modify the expression of MMP2 and -9 in astrocytes. Astrocytes were exposed to Aβ1-42 (Aβ, 2 μM) for 18 h. The expression of both MMP9 (a) and MMP2 (b), was evaluated. The treatment was not able to induce modifications in the expression of the protein. Data are mean ± SEM of 3 experiments Significance was assessed by Student's *t* test.

Figure S4. Aβ treatment did not modify the expression and the activity of MMP2 in endothelial cells. Both endothelial-astrocytes co-cultures and endothelial monolayers were exposed to Aβ 2 μM for 18 h. The medium released by endothelial cells following exposure to Aβ either in the presence of astrocytes (a) or in monoculture (b) was subjected to gelatin zymography assay to evaluate MMP2 enzymatic activity. No modification in the activity of the gelatinase was observed. In c (qRT-PCR) and d (western blot) expression of MMP2 in endothelial cells exposed to Aβ 2 μM in the presence of ACM Aβ, is shown. The release and activity of the protease was evaluated by processing endothelial culture media in a gelatin zymography assay (e). Values are expressed as percent of control. Data are mean ± SEM of 3 experiments. Significance was assessed by Student's *t*-test.

References

Abbott N. J., Ronnback L. and Hansson E. (2006) Astrocyte-endothelial interactions at the blood-brain barrier. *Nat. Rev. Neurosci.* **7**, 41–53.

Alluri H., Wilson R. L., Anasooya Shaji C., *et al.* (2016) Melatonin preserves blood-brain barrier integrity and permeability via matrix metalloproteinase-9 inhibition. *PLoS ONE* **11**, e0154427.

Argaw A. T., Asp L., Zhang J., Navrazhina K., Pham T., Mariani J. N., *et al.* (2012) Astrocyte-derived VEGF-A drives blood-brain barrier

disruption in CNS inflammatory disease. *J. Clin. Investig.* **122**, 2454–2468.

Batarseh Y. S., Duong Q. V., Mousa Y. M., Al Rihani S.B., Elfakhri K and Kaddoumi A. (2016) Amyloid-beta and astrocytes interplay in amyloid-beta related disorders. *Int. J. Mol. Sci.* **17**, 338.

Bell R. D. and Zlokovic B. V. (2009) Neurovascular mechanisms and blood-brain barrier disorder in Alzheimer's disease. *Acta Neuropathol.* **118**, 103–113.

Brkic M., Balusu S., Van Wonterghem E., Gorle N., Benilova I., Kremer A., *et al.* (2015) Amyloid beta oligomers disrupt blood-CSF barrier integrity by activating matrix metalloproteinases. *J. Neurosci.* **35**, 12766–12778.

Capaldo C. T. and Nusrat A. (2009) Cytokine regulation of tight junctions. *Biochem. Biophys. Acta.* **1788**:864–871.

Chapouly C., Tadesse Argaw A., Horng S., Castro K., Zhang J., Asp L., *et al.* (2015) Astrocytic TYMP and VEGFA drive blood-brain barrier opening in inflammatory central nervous system lesions. *Brain* **138**(Pt 6):1548–1567.

Cheslow L. and Alvarez J. I. (2016) Glial-endothelial crosstalk regulates blood-brain barrier function. *Curr. Opin. Pharmacol.* **26**, 39–46.

Dal Pra. I., Armato U., Chioffi F., Pacchiana R., Whitfield J. F., Chakravarthy B., *et al.* (2014) The Abeta peptides-activated calcium-sensing receptor stimulates the production and secretion of vascular endothelial growth factor-A by normoxic adult human cortical astrocytes. *NeuroMol. Med.* **16**, 645–657.

Di Marco L. Y., Venneri A., Farkas E., Evans P. C., Marzo A. and Frangi A. F. (2015) Vascular dysfunction in the pathogenesis of Alzheimer's disease - A review of endothelium-mediated mechanisms and ensuing vicious circles. *Neurobiol. Dis.* **82**, 593–606.

Fujimoto M., Takagi Y., Aoki T., Hayase M., Marumo T., Gomi M., *et al.* (2008) Tissue inhibitor of metalloproteinases protect blood-brain barrier disruption in focal cerebral ischemia. *J. Cereb. Blood Flow Metab.* **28**, 1674–1685.

Garcia K. O., Ornellas F. L., Martin P. K., Patti C. L., Mello L. E., Frussa-Filho R., *et al.* (2014) Therapeutic effects of the transplantation of VEGF overexpressing bone marrow mesenchymal stem cells in the hippocampus of murine model of Alzheimer's disease. *Front. Aging Neurosci.* **6**, 30.

Garwood C. J., Ratcliffe L. E., Simpson J. E., Heath P. R., Ince P. G. and Wharton S. B. (2016) Review: astrocytes in Alzheimer's disease and other age-associated dementias; a supporting player with a central role. *Neuropathol. Appl. Neurobiol.* doi: 10.1111/nan.12338. [Epub ahead of print].

Gheorghiu M., Enciu A. M., Popescu B. O. and Gheorghiu E. (2014) Functional and molecular characterization of the effect of amyloid-beta42 on an in vitro epithelial barrier model. *J. Alzheimer's Dis.* **38**, 787–798.

Gonzalez-Velasquez F. J., Kotarek J. A. and Moss M. A. (2008) Soluble aggregates of the amyloid-beta protein selectively stimulate permeability in human brain microvascular endothelial monolayers. *J. Neurochem.* **107**, 466–477.

van de Haar H. J., Burgmans S., Jansen J. F., van Osch M. J., van Buchem M. A., Muller M., *et al.* (2016) Blood-brain barrier leakage in patients with early Alzheimer disease. *Radiology* **281**, 527–535.

Haruki H., Sano Y., Shimizu F., Omoto M., Tasaki A., Oishi M., *et al.* (2013) NMO sera down-regulate AQP4 in human astrocyte and induce cytotoxicity independent of complement. *J. Neurol. Sci.* **331**, 136–144.

Hollborn M., Stathopoulos C., Steffen A., Wiedemann P., Kohen L. and Bringmann A. (2007) Positive feedback regulation between MMP-9 and VEGF in human RPE cells. *Invest. Ophthalmol. Vis. Sci.* **48**, 4360–4367.

Jellinger K. A. and Attems J. (2005) Prevalence and pathogenic role of cerebrovascular lesions in Alzheimer disease. *J. Neurol. Sci.* **229–230**, 37–41.

Jo W. K., Law A. C. and Chung S. K. (2014) The neglected co-star in the dementia drama: the putative roles of astrocytes in the pathogeneses of major neurocognitive disorders. *Mol. Psychiatry* **19**, 159–167.

Keller A. (2013) Breaking and building the wall: the biology of the blood-brain barrier in health and disease. *Swiss Med. Wkly* **143**, w13892.

Kim J. Y., Ko A. R., Hyun H. W. and Kang T. C. (2015) ETB receptor-mediated MMP-9 activation induces vasogenic edema via ZO-1 protein degradation following status epilepticus. *Neuroscience* **304**, 355–367.

Koch S., Tugues S., Li X., Gualandi L. and Claesson-Welsh L. (2011) Signal transduction by vascular endothelial growth factor receptors. *Biochem. J.* **437**, 169–183.

Kook S. Y., Hong H. S., Moon M., Ha C. M., Chang S. and Mook-Jung I. (2012) Abeta(1)(-)(4)(2)-RAGE interaction disrupts tight junctions of the blood-brain barrier via Ca(2)(+)-calcineurin signaling. *J. Neurosci.* **32**, 8845–8854.

Lamoke F., Mazzone V., Persichini T., Maraschi A., Harris M. B., Venema R. C., *et al.* (2015) Amyloid beta peptide-induced inhibition of endothelial nitric oxide production involves oxidative stress-mediated constitutive eNOS/HSP90 interaction and disruption of agonist-mediated Akt activation. *J. Neuroinflammation* **12**, 84.

Liu R., Zhang T. T., Wu C. X., Lan X. and Du G. H. (2011) Targeting the neurovascular unit: development of a new model and consideration for novel strategy for Alzheimer's disease. *Brain Res. Bull.* **86**, 13–21.

Maharaj A. S. and D'Amore P. A. (2007) Roles for VEGF in the adult. *Microvasc. Res.* **74**, 100–113.

Marco S. and Skaper S. D. (2006) Amyloid beta-peptide1-42 alters tight junction protein distribution and expression in brain microvessel endothelial cells. *Neurosci. Lett.* **401**, 219–224.

Merlo S. and Sortino M. A. (2012) Estrogen activates matrix metalloproteinases-2 and -9 to increase beta amyloid degradation. *Mol. Cell Neurosci.* **49**, 423–429.

Mizee M. R., Nijland P. G., van der Pol S. M., Drexhage J. A., van Het Hof B., Mebius R., *et al.* (2014) Astrocyte-derived retinoic acid: a novel regulator of blood-brain barrier function in multiple sclerosis. *Acta Neuropathol.* **128**, 691–703.

Munaut C., Noel A., Hougrand O., Foidart J. M., Boniver J. and Deprez M. (2003) Vascular endothelial growth factor expression correlates with matrix metalloproteinases MT1-MMP, MMP-2 and MMP-9 in human glioblastomas. *Int. J. Cancer* **106**, 848–855.

Nagababu E., Usatyuk P. V., Enika D., Natarajan V. and Rifkind J. M. (2009) Vascular endothelial barrier dysfunction mediated by amyloid-beta proteins. *J. Alzheimer's Dis.* **17**, 845–854.

Nair A., Frederick T. J. and Miller S. D. (2008) Astrocytes in multiple sclerosis: a product of their environment. *Cell. Mol. Life Sci.* **65**, 2702–2720.

Ortiz G. G., Pacheco-Moises F. P., Macias-Islas M. A., Flores-Alvarado L. J., Mireles-Ramirez M. A., Gonzalez-Renovato E. D., *et al.* (2014) Role of the blood-brain barrier in multiple sclerosis. *Arch. Med. Res.* **45**, 687–697.

Park S. W., Kim J. H., Mook-Jung I., Kim K. W., Park W. J., Park K. H., *et al.* (2014a) Intracellular amyloid beta alters the tight junction of retinal pigment epithelium in 5XFAD mice. *Neurobiol. Aging* **35**, 2013–2020.

Park R., Kook S. Y., Park J. C. and Mook-Jung I. (2014b) Abeta1-42 reduces P-glycoprotein in the blood-brain barrier through RAGE-NF-kappaB signaling. *Cell Death Dis.* **5**, e1299.

Park J. C., Baik S. H., Han S. H., Cho H. J., Choi H., Kim H. J., *et al.* (2016) Annexin A1 restores Abeta1-42 -induced blood-brain barrier disruption through the inhibition of RhoA-ROCK signaling pathway. *Aging Cell*.

Ries M. and Sastre M. (2016) Mechanisms of abeta clearance and degradation by glial cells. *Front. Aging Neurosci.* **8**, 160.

Sagare A. P., Bell R. D. and Zlokovic B. V. (2012) Neurovascular dysfunction and faulty amyloid beta-peptide clearance in Alzheimer disease. *Cold Spring Harb. Perspect Med.* **2**, 10.

Sano Y., Shimizu F., Abe M., Maeda T., Kashiwamura Y., Ohtsuki S., *et al.* (2010) Establishment of a new conditionally immortalized human brain microvascular endothelial cell line retaining an in vivo blood-brain barrier function. *J. Cell. Physiol.* **225**, 519–528.

Sano Y., Kashiwamura Y., Abe M., Dieu L.-H., Huwyler J., Shimizu F., *et al.* (2013) Stable human brain microvascular endothelial cell line retaining its barrier-specific nature independent of the passage number. *Clin. Exp. Neuroimmunol.* **4**, 92–103.

Spampinato S. F., Obermeier B., Cotleur A., Love A., Takeshita Y., Sano Y., *et al.* (2015) Sphingosine 1 phosphate at the blood brain barrier: can the modulation of S1P receptor 1 Influence the response of endothelial cells and astrocytes to inflammatory stimuli? *PLoS ONE* **10**, e0133392.

Tai L. M., Holloway K. A., Male D. K., Loughlin A. J. and Romero I. A. (2010) Amyloid-beta-induced occludin down-regulation and increased permeability in human brain endothelial cells is mediated by MAPK activation. *J. Cell Mol. Med.* **14**, 1101–1112.

Tasaki A., Shimizu F., Sano Y., Fujisawa M., Takahashi T., Haruki H., *et al.* (2014) Autocrine MMP-2/9 secretion increases the BBB permeability in neuromyelitis optica. *J. Neurol. Neurosurg. Psychiatry* **85**, 419–430.

Thirumangalakudi L., Samany P. G., Owoso A., Wiskar B. and Grammas P. (2006) Angiogenic proteins are expressed by brain blood vessels in Alzheimer's disease. *J. Alzheimer's Dis.* **10**, 111–118.

de la Torre J. C. (2002) Alzheimer disease as a vascular disorder: nosological evidence. *Stroke* **33**, 1152–1162.

Valable S., Montaner J., Bellail A., Berezowski V., Brillault J., Cecchelli R., *et al.* (2005) VEGF-induced BBB permeability is associated with an MMP-9 activity increase in cerebral ischemia: both effects decreased by Ang-1. *J. Cereb. Blood Flow Metab.* **25**, 1491–1504.

Wan W., Cao L., Liu L., Zhang C., Kalionis B., Tai X., *et al.* (2015) Abeta oligomer-induced leakage in an in vitro blood brain barrier model is associated with upregulation of RAGE and metalloproteinases, and downregulation of tight junction scaffold proteins. *J. Neurochem.* **134**, 382–393.

Wang J. Z., Zhu W. D., Xu Z. X., Du W. T., Zhang H. Y., Sun X. W., *et al.* (2014) Pin1, endothelial nitric oxide synthase, and amyloid-beta form a feedback signaling loop involved in the pathogenesis of Alzheimer's disease, hypertension, and cerebral amyloid angiopathy. *Med. Hypotheses* **82**, 145–150.

Xin H., Liang W., Mang J., Lin L., Guo N., Zhang F., *et al.* (2012) Relationship of gelatinases-tight junction proteins and blood-brain barrier permeability in the early stage of cerebral ischemia and reperfusion. *Neural Regen. Res.* **7**, 2405–2412.

Yang Y., Estrada E. Y., Thompson J. F., Liu W. and Rosenberg G. A. (2007) Matrix metalloproteinase-mediated disruption of tight junction proteins in cerebral vessels is reversed by synthetic matrix metalloproteinase inhibitor in focal ischemia in rat. *J. Cereb. Blood Flow Metab.* **27**, 697–709.

Yang J., Wang G., Gao C., Shao G. and Kang N. (2013) Effects of hyperbaric oxygen on MMP-2 and MMP-9 expression and spinal cord edema after spinal cord injury. *Life Sci.* **93**, 1033–1038.

Zand L., Ryu J. K. and McLarnon J. G. (2005) Induction of angiogenesis in the beta-amyloid peptide-injected rat hippocampus. *NeuroReport* **16**, 129–132.

Zenaro E., Piacentino G. and Constantin G. (2016) The blood-brain barrier in Alzheimer's disease. *Neurobiol. Dis.* pii: S0969-9961(16)30165-6. doi: 10.1016/j.nbd.2016.07.007. [Epub ahead of print].

Zhao Z., Nelson A. R., Betsholtz C. and Zlokovic B. V. (2015) Establishment and dysfunction of the blood-brain barrier. *Cell* **163**, 1064–1078.